Control of quantized photon states with cascade phase conjugators by modulation pumping

Tsuyoshi Fukuo
Department of Applied Physics, Osaka City University, Sugimoto, Sumiyoshi-ku, Osaka 558, Japan

Tetsuo Ogawa
Department of Physics, Tohoku University, Aoba-ku, Sendai 980-77, Japan

(Received 17 September 1997)

Squeezing properties of a quantized photon field interacting with *cascade* four-wave-mixing materials (phase conjugators) are investigated theoretically by the transfer-matrix method. The controllability of the quantum fluctuation of the photon field is improved with the use of modulation pumping, in which phases of pumping beams of the phase conjugators are individually controlled even when their optical nonlinearity and/or the pumping power are fixed. By choosing appropriate numbers of phase conjugators and phase differences of the pump beams, incident coherent light is transformed to quadrature-phase-amplitude (QPA) squeezed states and photon-number-squeezed states. Optimal squeezing of both the QPA and photon number can be realized with this cascade system by modulation pumping. Partial (normal) reflection of light at surfaces of the phase conjugators is shown quantitatively to suppress the squeezing. Comparison with an ordinary method using a single-phase conjugator is also made. [S1050-2947(98)02603-1]

PACS number(s): 42.50.Dv, 42.50.Ar, 42.65.−k

I. INTRODUCTION

The generation of squeezed states, which have less noise than the coherent state in one of the canonical conjugate variables in an electromagnetic field still satisfying the minimum uncertainty relation [1], has been studied in many models, especially using the nonlinear optical interactions, e.g., parametric amplifiers [2,3], four-wave mixings (FWM's) [4–6], optical Kerr effects [7], and others. The squeezed state is expected to have a potential for applications in quantum optical communication or gravity-wave detectors. However, these schemes require a very large optical nonlinearity of the materials and/or strong pumping power to obtain the squeezed light. Thus we had poor controllability of the squeezing of the photon field in actual experiments. A main point of this paper is to present a scheme for the generation of squeezed states with fine controllability.

Yurke [8] proposed an improved scheme for generation of the quadrature-phase amplitude (QPA) squeezed state of light, which makes use of the phase-conjugation process in a cavity [9–11]. His model consists of a cavity-containing *single* FWM medium and a perfect mirror, which is called the phase-conjugation cavity (PCC), and the squeezed light is generated efficiently by the resonance effect in the cavity FWM process [Fig. 1(a)]. Our proposed scheme is an extension of the Yurke's model, cutting up the single FWM medium into several pieces to form *cascade* phase conjugators, as shown in Fig. 1(b) [12]. We will show that with our scheme the controllability of the squeezing is improved by introducing additional control parameters, phases of pumping beams of each nonlinear media, which are controllable independently. This is the method of modulation pumping for controlling the squeezed states of light. We will investigate theoretically in detail the squeezing of the QPA and of the photon number by the transfer-matrix method. General formulas for the QPA variance and the Fano factor of an output light are analytically given, which depend sensitively on the pump phase differences and on the number of phase conjugators.

This paper is organized as follows. In Sec. II, our cascade model is introduced after a brief review of Yurke's model. We employ the transfer-matrix method and analyze the cascade systems generally to obtain the input-output relation of a quantized photon field. Section III is devoted to a discussion of the quantum fluctuations of the output light for particular cases as examples in terms of the QPA squeezing and the photon-number squeezing. Effects of normal reflection at surfaces and interfaces of nonlinear media are studied in Sec. IV.

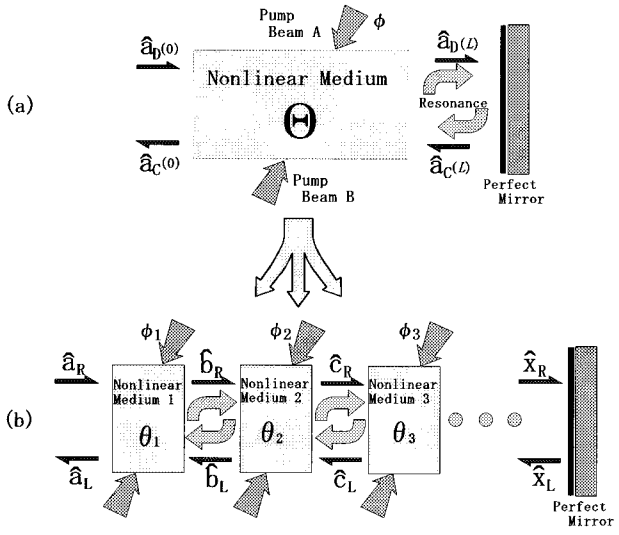

FIG. 1. Schematic drawing of two schemes for optical squeezing with the use of the phase-conjugation cavity (PCC), which consists of one or more FWM media and a perfect mirror; (a) Yurke's model and (b) our model.

II. CASCADE MODEL AND THE INPUT-OUTPUT RELATIONS

A. Brief review of Yurke's model

Both Yurke's model and our model make use of phase-conjugation processes in third-order optical nonlinear material(s). At first we shall review Yurke's model corresponding to the case of a single-phase conjugator (its length L), as shown in Fig. 1(a). Two counterpropagating pump beams are labeled by suffixes A and B, and two signal beams by C and D. We assume that the pump beams are treated classically, and that photoabsorption in the media is negligible. Then the FWM process in the nonlinear material is described by an input-output relation; output lights from the nonlinear medium, $\hat{a}_C(0)$ and $\hat{a}_D(L)$, are represented by the input lights, $\hat{a}_C(L)$ and $\hat{a}_D(0)$, as [8,12]

$$\hat{a}_C(0)=\mu\hat{a}_C(L)+\nu\hat{a}_D^{\dagger}(0), \tag{1}$$

$$\hat{a}_D(L)=\mu\hat{a}_D(0)+\nu\hat{a}_C^{\dagger}(L), \tag{2}$$

where $\mu\equiv\sec\Theta$ and $\nu\equiv e^{i\phi}\tan\Theta$ characterize the nonlinearity of the FWM process. Here

$$\Theta=\mathrm{Re}[\chi^{(3)}]E_AE_BL, \tag{3}$$

$$\phi=\phi_A^{\mathrm{pump}}+\phi_B^{\mathrm{pump}}. \tag{4}$$

The former is a phase angle describing the nonlinearity of the phase conjugator, which is determined by the third-order nonlinear susceptibility $\chi^{(3)}$, the pumping strength E_AE_B, and the interaction length L. The latter is the sum of the phases of pump beams, which are described by complex amplitudes $E_A\exp(i\phi_A^{\mathrm{pump}})$ and $E_B\exp(i\phi_B^{\mathrm{pump}})$, with real amplitudes, E_A and E_B. Here we note that the unitarity condition $|\mu|^2-|\nu|^2=1$ is satisfied.

At one end of the cavity in Fig. 1(a), we employ the boundary condition $\hat{a}_C(L)=\hat{a}_D(L)$, describing the effect of a perfect mirror. The output beam from the PCC, $\hat{a}_{\mathrm{out}}\equiv\hat{a}_C(0)$, is given by the linear combination of the annihilation and creation operators, $\hat{a}_{\mathrm{in}}\equiv\hat{a}_D(0)$ and $\hat{a}_{\mathrm{in}}^{\dagger}\equiv\hat{a}_D^{\dagger}(0)$, of the input beam as

$$\begin{aligned}\hat{a}_{\mathrm{out}}&=\frac{\mu^2}{2-\mu^2}\hat{a}_{\mathrm{in}}+\frac{2\nu}{2-\mu^2}\hat{a}_{\mathrm{in}}^{\dagger}=\hat{a}_{\mathrm{in}}\sec(2\Theta)+\hat{a}_{\mathrm{in}}^{\dagger}e^{i\phi}\tan(2\Theta)\\&\equiv\mu_{\mathrm{PCC}}^{(1)}\hat{a}_{\mathrm{in}}+\nu_{\mathrm{PCC}}^{(1)}\hat{a}_{\mathrm{in}}^{\dagger}.\end{aligned} \tag{5}$$

This is the input-output relation for Yurke's model. The unitarity relation $|\mu_{\mathrm{PCC}}^{(1)}|^2-|\nu_{\mathrm{PCC}}^{(1)}|^2=1$ still holds. The fluctuation of the normalized QPA's is then squeezed as

$$\begin{aligned}\langle\Delta\hat{q}_{\mathrm{out}}^2\rangle&\equiv\langle\alpha|\hat{q}_{\mathrm{out}}^2|\alpha\rangle-\langle\alpha|\hat{q}_{\mathrm{out}}|\alpha\rangle^2=|\mu_{\mathrm{PCC}}^{(1)}|^2+|\nu_{\mathrm{PCC}}^{(1)}|^2\\&\quad-2|\mu_{\mathrm{PCC}}^{(1)}\nu_{\mathrm{PCC}}^{(1)}|\leqslant 1,\end{aligned} \tag{6}$$

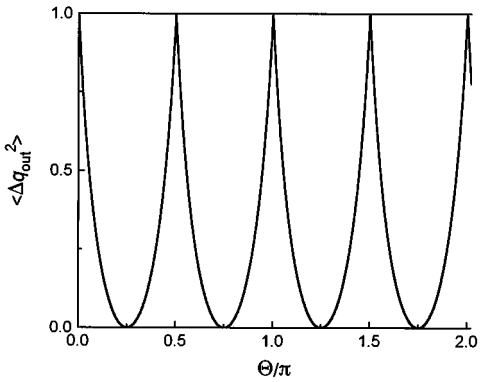

FIG. 2. The QPA variance $\langle\Delta\hat{q}_{\mathrm{out}}^2\rangle$ is plotted as a function of the nonlinear parameter Θ in Yurke's model ($N=1$).

$$\langle\Delta\hat{p}_{\mathrm{out}}^2\rangle=|\mu_{\mathrm{PCC}}^{(1)}|^2+|\nu_{\mathrm{PCC}}^{(1)}|^2+2|\mu_{\mathrm{PCC}}^{(1)}\nu_{\mathrm{PCC}}^{(1)}|\geqslant 1, \tag{7}$$

where $\hat{q}_{\mathrm{out}}\equiv\hat{a}_{\mathrm{out}}+\hat{a}_{\mathrm{out}}^{\dagger}$ and $\hat{p}_{\mathrm{out}}\equiv(\hat{a}_{\mathrm{out}}-\hat{a}_{\mathrm{out}}^{\dagger})/i$. Here the incident light is assumed to be the coherent state $|\alpha\rangle$, defined by $\hat{a}_{\mathrm{in}}|\alpha\rangle=\alpha|\alpha\rangle$, and the squeezing angle ϕ_{SA} is chosen to be

$$\phi_{\mathrm{SA}}\equiv\tfrac{1}{2}(\arg\mu_{\mathrm{PCC}}^{(1)}+\arg\nu_{\mathrm{PCC}}^{(1)})=\frac{\pi}{2}, \tag{8}$$

to minimize $\langle\Delta\hat{q}_{\mathrm{out}}^2\rangle$ and hence to maximize $\langle\Delta\hat{p}_{\mathrm{out}}^2\rangle$. It is of course possible to squeeze the $\hat{p}_{\mathrm{out}}$ component by adjusting ϕ_{SA}. However, when we discuss the QPA squeezing, squeezing for the $\hat{q}_{\mathrm{out}}$ component ($\langle\Delta\hat{q}_{\mathrm{out}}^2\rangle\leqslant 1$) is always considered by adjusting ϕ_{SA}. Here we note that these QPA variances are independent of the number of incident photons, $|\alpha|^2$, and the uncertainty product satisfies the minimum uncertainly relation $\langle\Delta\hat{q}_{\mathrm{out}}^2\rangle\langle\Delta\hat{p}_{\mathrm{out}}^2\rangle=1$. The QPA variance $\langle\Delta\hat{q}_{\mathrm{out}}^2\rangle$ is a function of the coupling constant Θ, as shown in Fig. 2. In Yurke's model, $\langle\Delta\hat{q}_{\mathrm{out}}^2\rangle$ is minimized, to vanish (the infinite squeezing) at $\Theta=(2m+1)\pi/4$ for $m=0,1,2,\ldots$.

B. Our model and the transfer-matrix method

In our model, the cavity has more than one ($N\geqslant 2$) phase conjugator, with the nonlinear coupling constants θ_i ($i=1,2,\ldots,N$), as shown in Fig. 1(b). For fair comparison with Yurke's model, we set

$$\sum_{i=1}^{N}\theta_i=\Theta, \tag{9}$$

and $\theta_i=\theta$. This means that the total nonlinearity of many nonlinear media is chosen to be the same as that in Yurke's model. Actually, we assume that $\mathrm{Re}[\chi^{(3)}]$ and the pumping power E_i^2 are identical with one another for N phase conju-

gators, and they are also the same as those in Yurke's model. Hence $\Sigma_{i=1}^{N} L_i = L$ is assumed (e.g., $L_i = L/N$), where L_i is the interaction length of the ith material.

To analyze this model, the transfer-matrix method is employed. The FWM process in the $(i=1)$th nonlinear medium in Fig. 1(b) is described as

$$\hat{a}_L = \hat{b}_L \sec\,\theta_i + \hat{a}_R^{\dagger} e^{i\phi_i} \tan\,\theta_i , \tag{10}$$

$$\hat{b}_R = \hat{a}_R \sec\,\theta_i + \hat{b}_L^{\dagger} e^{i\phi_i} \tan\,\theta_i , \tag{11}$$

where ϕ_i is the sum of phases of two counterpropagating pump beams for the ith medium. Equations (10) and (11) are represented in matrix notation as

$$\begin{pmatrix} \hat{a}_L \\ \hat{a}_R^{\dagger} \end{pmatrix} = \frac{1}{\mu_i} \begin{pmatrix} 1 & \nu_i \\ -\nu_i^{*} & 1 \end{pmatrix} \begin{pmatrix} \hat{b}_L \\ \hat{b}_R^{\dagger} \end{pmatrix}, \tag{12}$$

or $\mathbf{A} = \mathbf{M}_i \mathbf{B}$ with $\mu_i \equiv \sec\,\theta_i$ and $\nu_i \equiv e^{i\phi_i} \tan\,\theta_i$. In the case where N nonlinear media exist, as shown in Fig. 1(b), Eq. (12) is extended to

$$\begin{pmatrix} \hat{a}_L \\ \hat{a}_R^{\dagger} \end{pmatrix} \equiv \mathbf{A} = \left[\prod_{i=1}^{N} \mathbf{M}_i \right] \mathbf{X} \equiv \mathbf{T}\mathbf{X} = \begin{pmatrix} t_{11}^{(N)} & t_{12}^{(N)} \\ t_{21}^{(N)} & t_{22}^{(N)} \end{pmatrix} \begin{pmatrix} \hat{x}_L \\ \hat{x}_R^{\dagger} \end{pmatrix}. \tag{13}$$

Using the boundary condition $\hat{x}_L = \hat{x}_R$, the input-output relation becomes

$$\hat{a}_{\rm out} = \frac{1}{|t_{11}^{(N)}|^2 - |t_{12}^{(N)}|^2} \hat{a}_{\rm in} + \frac{2 t_{11}^{(N)} t_{12}^{(N)}}{|t_{11}^{(N)}|^2 - |t_{12}^{(N)}|^2} \hat{a}_{\rm in}^{\dagger} \equiv \mu_{\rm PCC}^{(N)} \hat{a}_{\rm in} + \nu_{\rm PCC}^{(N)} \hat{a}_{\rm in}^{\dagger}. \tag{14}$$

This is one of the general results in this paper. The matrix elements $t_{11}^{(N)}$ and $t_{12}^{(N)}$ are analytically given as

$$t_{11}^{(N)} = \cos^N \theta \sum_{n=0}^{N-1} \left\{ (-1)^n \tan^{2n}\theta \times \sum^{*} \exp\left[i \sum_{m=0}^{2n} (-1)^{m+1} \phi_m \right] \right\}$$
$$= \cos^N \theta \left[1 - \tan^2 \theta \sum_{i<j} e^{i(\phi_i - \phi_j)} + \tan^4 \theta \sum_{i<j<k<l} e^{i(\phi_i - \phi_j + \phi_k - \phi_l)} - \cdots \right], \tag{15}$$

$$t_{12}^{(N)} = \cos^N \theta \sum_{n=0}^{N-1} \left\{ (-1)^n \tan^{2n+1}\theta \times \sum^{**} \exp\left[i \sum_{m=1}^{2n+1} (-1)^{m+1} \phi_m \right] \right\}$$
$$= \cos^N \theta \left[\tan\,\theta \sum_i e^{i\phi_i} - \tan^3\theta \sum_{i<j<k} e^{i(\phi_i - \phi_j + \phi_k)} + \tan^5 \theta \sum_{i<j<k<l<m} e^{i(\phi_i - \phi_j + \phi_k - \phi_l + \phi_m)} - \cdots \right], \tag{16}$$

where $\phi_0 = 0$ and

$$\sum^{*} \equiv \underbrace{\sum_{i<j<\cdots}^{2n \le N}}_{2n}, \tag{17}$$

$$\sum^{**} \equiv \underbrace{\sum_{i<j<\cdots}^{2n+1 \le N}}_{2n+1}. \tag{18}$$

In Eq. (14), the unitarity condition $|\mu_{\rm PCC}^{(N)}|^2 - |\nu_{\rm PCC}^{(N)}|^2 = 1$ is satisfied if each nonlinear medium satisfies $|\mu_i|^2 - |\nu_i|^2 = 1$.

Here we note that free propagation of the electromagnetic wave in the vacuum from one nonlinear medium to the neighbor causes the phase change, described by the vacuum matrix

$$\mathbf{V}_{ij} \equiv \begin{pmatrix} e^{i\vartheta_{ij}} & 0 \\ 0 & e^{i\vartheta_{ij}} \end{pmatrix}. \tag{19}$$

Here $\vartheta_{ij} = k_0 l_{ij} = 2\pi l_{ij}/\lambda_0$, with the spatial separation between the ith and $j(=i\pm1)$th media l_{ij}, and $\lambda_0 = 2\pi/k_0$ is the wavelength of the light in the vacuum. In the following, we do not have to take care of this phase change because the phase changes of leftward-propagating and rightward-propagating light are counteracted by each other due to the perfect phase-conjugate reflection. Then insertion of $\mathbf{V}_{ij}$ into Eq. (13) leads to no change in $\langle \Delta \hat{q}_{\rm out}^2 \rangle$ and $\langle \Delta \hat{p}_{\rm out}^2 \rangle$.

III. SQUEEZING PROPERTIES IN THE $N=2$ AND 3 CASES

A. Quadrature-phase amplitude (QPA) squeezing

In this section, we calculate the QPA variance of the photon field with the use of the general result [Eq. (14)] for the $N=2$ and 3 cases as examples. In these cases, $\mu_{\rm PCC}^{(2)}$ and $\mu_{\rm PCC}^{(3)}$ are calculated as

$$\mu_{\rm PCC}^{(2)} \equiv [\,|t_{11}^{(2)}|^2 - |t_{12}^{(2)}|^2\,]^{-1} = \frac{\sec^2 2\theta}{1 - \tan^2 2\theta \cos\,\phi_{21}}, \tag{20}$$

$$\mu_{\mathrm{PCC}}^{(3)} \equiv [\,|t_{11}^{(3)}|^2 - |t_{12}^{(3)}|^2\,]^{-1} = \frac{\sec^3 2\theta}{1-\tan^2 2\theta[\cos\,\phi_{21}+\cos\,\phi_{23}-\sec 2\theta\,\cos(\phi_{21}+\phi_{23})+2\sec 2\theta\,\cos\,\phi_{21}\,\cos\,\phi_{23}/\sec^2\,\theta]}, \tag{21}$$

where $\phi_{ij} \equiv \phi_i - \phi_j$ is the pump phase difference between the ith and jth phase conjugators. As shown in Eqs. (20) and (21), ϕ_{ij}'s work as additional control parameters, and appear only in our model [i.e., ϕ_{21} for $N=2$ and (ϕ_{21},ϕ_{23}) for $N=3$]. One QPA variance $\langle \Delta \hat{q}_{\mathrm{out}}^2 \rangle$ is written in terms only of $\mu_{\mathrm{PCC}}^{(N)}$ as

$$\langle \Delta \hat{q}_{\mathrm{out}}^2 \rangle = 2|\mu_{\mathrm{PCC}}^{(N)}|^2 (1 - \sqrt{1-|\mu_{\mathrm{PCC}}^{(N)}|^{-2}}) - 1. \tag{22}$$

First, we shall consider the simplest cases of $\phi_{21}=0$ for $N=2$ and $\phi_{21}=\phi_{23}=0$ for $N=3$, where all nonlinear media have an identical coupling constant and the pump phases are the same as one another (no modulation pumping). In these cases, the squeezing parameters are reduced to

$$\mu_{\mathrm{PCC}}^{(2)} = \sec(4\theta) = \sec(2\Theta) \quad \text{for} \quad N=2, \tag{23}$$

$$\mu_{\mathrm{PCC}}^{(3)} = \sec(6\theta) = \sec(2\Theta) \quad \text{for} \quad N=3. \tag{24}$$

As they should be, these are the same as the result of Yurke's model; that is, without the modulation pumping, the cascade configuration of the phase conjugators plays no role in the enhancement of the QPA squeezing under the condition of Eq. (9).

Next, we shall investigate the role of the modulation pumping, i.e., nonzero ϕ_{ij}'s, in the QPA squeezing. In experiments, one can independently control the phase difference(s) ϕ_{21} and ϕ_{23}. Figure 3 shows $\langle \Delta \hat{q}_{\mathrm{out}}^2 \rangle$ as a function of ϕ_{21} and $\Theta = 2\theta$ for the $N=2$ case. When $(4m+1)\pi/4 < \Theta < (4m+3)\pi/4$ with $m=0,1,2,\ldots$, $\langle \Delta \hat{q}_{\mathrm{out}}^2 \rangle$ for $0 < \phi_{21} < \pi$ (with the modulation pumping) is smaller than that for $\phi_{21}=0$ (without the modulation pumping). Therefore, the finite phase difference of the pumping beams reduces the QPA variance for $\Theta \in [(4m+1)\pi/4, (4m+3)\pi/4]$. In other words, stronger squeezing is possible than in Yurke's model by the modulation pumping for such Θ. Otherwise [$0 < \Theta < \frac{1}{4}\pi$ and $(4m+3)\pi/4 < \Theta < (4m+5)\pi/4$]; however, QPA squeezing is suppressed by the modulation pumping. In the case of $N=3$, similarly, when $(6m+1)\pi/4 < \Theta < (6m+5)\pi/4$ with $m=0,1,2,\ldots$, $\langle \Delta \hat{q}_{\mathrm{out}}^2 \rangle$ for $0 < \phi_{21} < \pi$ and $0 < \phi_{23} < \pi$ is smaller than that for $\phi_{21} = \phi_{23} = 0$. In general, when $(2Nm+1)\pi/4 < \Theta < (2Nm+2N-1)\pi/4$ with $m=0,1,2,\ldots$, we can obtain stronger QPA squeezing by the modulation pumping ($\phi_{ij} \neq 0$) than that in the $\phi_{ij}=0$ case.

Figure 4(a) shows $\langle \Delta \hat{q}_{\mathrm{out}}^2 \rangle$ in the $N=3$ case as a function of ϕ_{21} and ϕ_{23} for $\theta = \frac{1}{6}\pi$ (i.e., $\Theta = \frac{1}{2}\pi$). In Fig. 4(b), solid

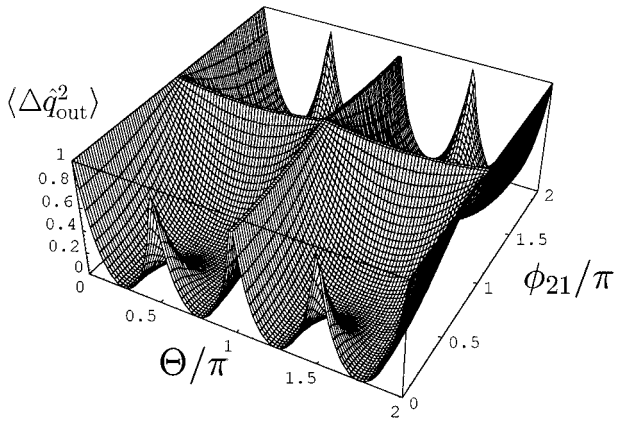

FIG. 3. The QPA variance $\langle \Delta \hat{q}_{\mathrm{out}}^2 \rangle$ is plotted as a function of the nonlinear parameter Θ and the pump phase difference ϕ_{21} in the case of $N=2$.

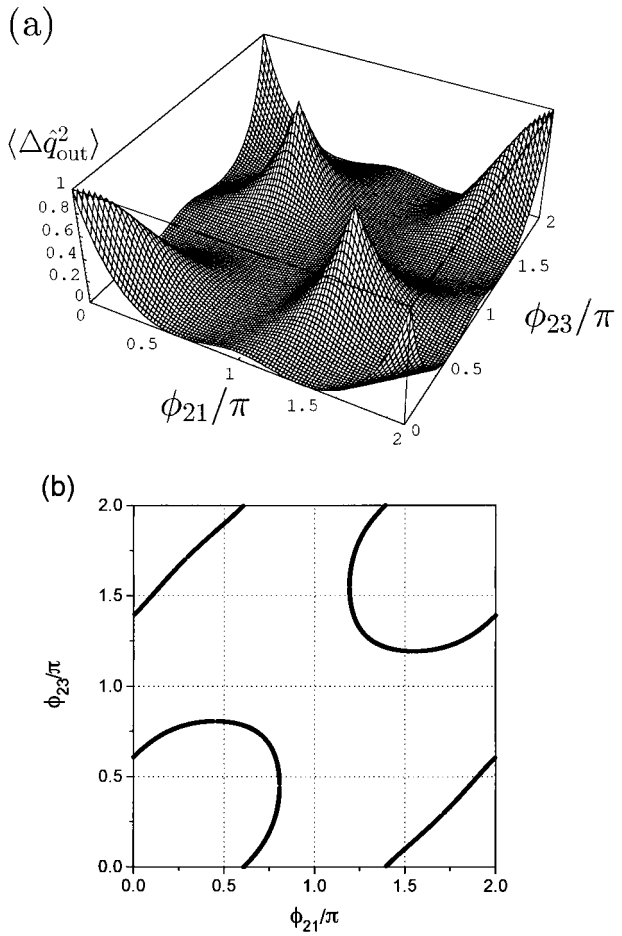

FIG. 4. (a) The QPA variance $\langle \Delta \hat{q}_{\mathrm{out}}^2 \rangle$ is plotted as a function of two pump phase differences ϕ_{21} and ϕ_{23} in the case of $N=3$. The nonlinear parameter is fixed to be $\Theta = \frac{1}{2}\pi$, i.e., $\theta = \frac{1}{6}\pi$. (b) The solid lines indicate a set of ϕ_{21} and ϕ_{23}, for which the infinite squeezing ($\langle \Delta \hat{q}_{\mathrm{out}}^2 \rangle = 0$) takes place, corresponding to the bottom of the ravines in (a).

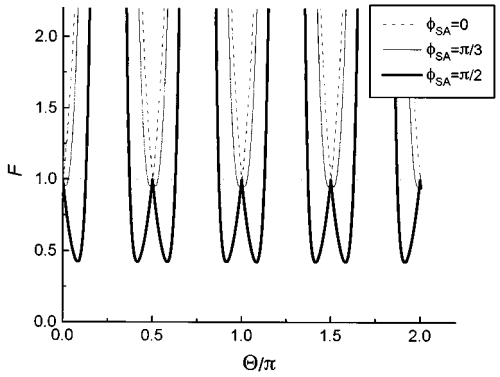

FIG. 5. The Fano factor F in the $N=1$ case (Yurke's model) is plotted as a function of the nonlinear parameter Θ for several values of the squeezing angle $\phi_{\rm SA}=0$, $\frac{1}{3}\pi$, and $\frac{1}{2}\pi$. The initial mean photon number is chosen to be $n_0=25$.

lines indicate a set of (ϕ_{21},ϕ_{23}) which yields the infinite squeezing $\langle\Delta\hat{q}^2_{\rm out}\rangle=0$. One finds that the QPA variance varies from zero to unity by controlling (ϕ_{21},ϕ_{23}) even when $\Theta=3\theta=\frac{1}{2}\pi$ is fixed. Here we recall that Yurke's model results in no QPA squeezing ($\langle\Delta\hat{q}^2_{\rm out}\rangle=0$) for $\Theta=\frac{1}{2}\pi$. This is an advantage of our scheme for the fine controllability of the QPA squeezing. As a consequence of this finding, when $\Theta\geqslant\frac{1}{4}\pi$, the infinite squeezing ($\langle\Delta\hat{q}^2_{\rm out}\rangle=0$) is always possible by choosing appropriate pump phase differences (ϕ_{ij}'s $\neq0$) and the number of phase conjugators, $N\geqslant2$.

B. Photon-number squeezing

We shall show that our scheme is also able to create the photon-number squeezed states. When the incident light is in the coherent state $|\alpha\rangle$, the mean photon number $\langle\hat{n}_{\rm out}\rangle$ and the Fano factor F of the output light from the PCC are described, respectively, by $\mu^{(N)}_{\rm PCC}$ and $\nu^{(N)}_{\rm PCC}$ as

$$\langle\hat{n}_{\rm out}\rangle\equiv\langle\alpha|\hat{a}^\dagger_{\rm out}\hat{a}_{\rm out}|\alpha\rangle=|\beta|^2+|\nu^{(N)}_{\rm PCC}|^2, \tag{25}$$

$$F\equiv\frac{\langle\Delta\hat{n}^2_{\rm out}\rangle}{\langle\hat{n}_{\rm out}\rangle}=\frac{|[\mu^{(N)}_{\rm PCC}]^*\beta+\nu^{(N)}_{\rm PCC}\beta^*|^2+2|\mu^{(N)}_{\rm PCC}\nu^{(N)}_{\rm PCC}|^2}{|\beta|^2+|\nu^{(N)}_{\rm PCC}|^2}, \tag{26}$$

where $\beta\equiv\mu^{(N)}_{\rm PCC}\alpha+\nu^{(N)}_{\rm PCC}\alpha^*$. In the following, we pay attention only to the Fano factor F to discuss the photon-number squeezing.

First we consider the dependence of the Fano factor in Yurke's model on the squeezing angle $\phi_{\rm SA}$ [Eq. (8)] and the nonlinear parameter Θ. In Yurke's model, the Fano factor is expressed by three parameters: n_0, $\mu^{(1)}_{\rm PCC}=\sec(2\Theta)$, and $\phi_{\rm SA}$. The Fano factor is plotted in Fig. 5 as a function of Θ for several values of $\phi_{\rm SA}$ under $n_0=25$. We find that the Fano factor for $\phi_{\rm SA}=\frac{1}{2}\pi$ is smaller than that for $\phi_{\rm SA}\neq\frac{1}{2}\pi$. Thus we set $\phi_{\rm SA}=\frac{1}{2}\pi$ in the discussion of the photon-number squeezing. When α is assumed to be real and $\phi_{\rm SA}$ is chosen to be $\frac{1}{2}\pi$, $\langle\hat{n}_{\rm out}\rangle$ and F are reduced to

$$\langle\hat{n}_{\rm out}\rangle=n_0(|\mu^{(1)}_{\rm PCC}|-\sqrt{|\mu^{(1)}_{\rm PCC}|^2-1})^2+|\mu^{(1)}_{\rm PCC}|^2-1, \tag{27}$$

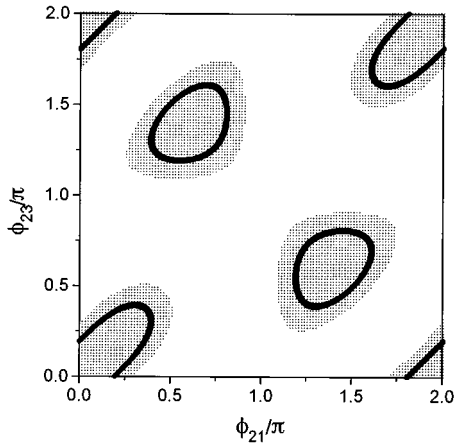

FIG. 6. The Fano factor is calculated on the plane of (ϕ_{21},ϕ_{23}) in the case of $N=3$ for $\Theta=\frac{1}{2}\pi$, $n_0=25$, and $\phi_{\rm SA}=\frac{1}{2}\pi$. In dotted regions, the photon statistics is of sub-Poissonian type ($F<1$). The Fano factor becomes minimum on the solid lines. A set of (ϕ_{21},ϕ_{23}) minimizing F differs from that minimizing $\langle\Delta\hat{q}^2_{\rm out}\rangle$. Compare with Fig. 4(b).

$$F=\frac{n_0(|\mu^{(1)}_{\rm PCC}|-\sqrt{|\mu^{(1)}_{\rm PCC}|^2-1})^4+2|\mu^{(1)}_{\rm PCC}|^2(|\mu^{(1)}_{\rm PCC}|^2-1)}{n_0(|\mu^{(1)}_{\rm PCC}|-\sqrt{|\mu^{(1)}_{\rm PCC}|^2-1})^2+|\mu^{(1)}_{\rm PCC}|^2-1}, \tag{28}$$

where $n_0\equiv|\alpha|^2$ is the mean photon number of the incident light. We note that in general the Fano factor becomes smaller for larger n_0.

The Fano factor in our cascade model ($N\geqslant2$) is readily obtained by replacing $\mu^{(1)}_{\rm PCC}$ in Eq. (28) by $\mu^{(N)}_{\rm PCC}$ given in Eqs. (14), (15), and (16). In the case of $N=3$ with $n_0=25$ and $\phi_{\rm SA}=\frac{1}{2}\pi$, the Fano factor is calculated as a function of ϕ_{21} and ϕ_{23} for $\Theta=\frac{1}{2}\pi$ ($\theta=\frac{1}{6}\pi$). A sub-Poissonian photon statistics ($F<1$) is possible in the dotted regions of Fig. 6. One finds that the photon statistics can be controlled from sub-Poissonian ($F<1$) to super-Poissonian ($F>1$) types simply by changing the pump phase differences.

Comparing Fig. 4(b) with Fig. 6, there seems to exist a relation between the QPA squeezing and the photon-number squeezing. Actually, the mean photon number and the Fano factor can be written in terms of $\langle\Delta\hat{q}^2_{\rm out}\rangle$ and n_0, that is,

$$\langle\hat{n}_{\rm out}\rangle=n_0\langle\Delta\hat{q}^2_{\rm out}\rangle+\frac{(1-\langle\Delta\hat{q}^2_{\rm out}\rangle)^2}{4\langle\Delta\hat{q}^2_{\rm out}\rangle}, \tag{29}$$

$$F=\frac{8n_0\langle\Delta\hat{q}^2_{\rm out}\rangle^4+(1-\langle\Delta\hat{q}^2_{\rm out}\rangle^2)^2}{8n_0\langle\Delta\hat{q}^2_{\rm out}\rangle^3+2\langle\Delta\hat{q}^2_{\rm out}\rangle(1-\langle\Delta\hat{q}^2_{\rm out}\rangle)^2}. \tag{30}$$

This relationship is independent of the details of μ and $\mu^{(N)}_{\rm PCC}$.

Figure 7 shows the relation between the QPA variance $\langle\Delta\hat{q}^2_{\rm out}\rangle$ and the Fano factor F for several values of n_0. One finds that the Fano factor diverges to infinity ($F\to\infty$) for excessive QPA squeezing ($\langle\Delta\hat{q}^2_{\rm out}\rangle\to0$), and only the Poissonian statistics ($F=1$) is possible for $\langle\Delta\hat{q}^2_{\rm out}\rangle\to1$. Then *moderate* QPA squeezing is required to yield optimal

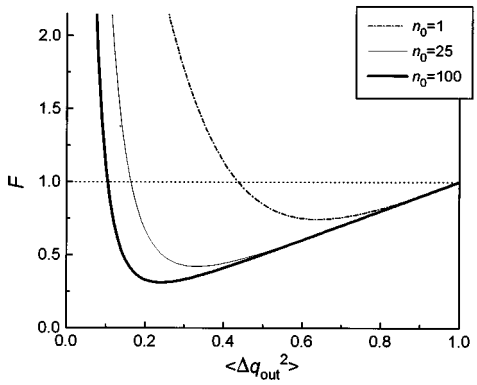

FIG. 7. Relation between the Fano factor F and the QPA variance $\langle \Delta \hat{q}_{\rm out}^2 \rangle$ for various values of n_0: $n_0=1$, 25, and 100. Here the squeezing angle $\phi_{\rm SA}$ is fixed to $\frac{1}{2}\pi$.

photon-number squeezing, i.e., to minimize F. There exists a lower bound for F in Fig. 7. The Fano factor reaches a minimum when n_0 and $\langle \Delta \hat{q}_{\rm out}^2 \rangle$ satisfy

$$32n_0\langle \Delta \hat{q}_{\rm out}^2 \rangle^4 (1-\langle \Delta \hat{q}_{\rm out}^2 \rangle + n_0 \langle \Delta \hat{q}_{\rm out}^2 \rangle^2) - 12 n_0 \langle \Delta \hat{q}_{\rm out}^2 \rangle^2 \times (1-\langle \Delta \hat{q}_{\rm out}^2 \rangle^4) - (1+\langle \Delta \hat{q}_{\rm out}^2 \rangle)(1-\langle \Delta \hat{q}_{\rm out}^2 \rangle)^5 = 0. \tag{31}$$

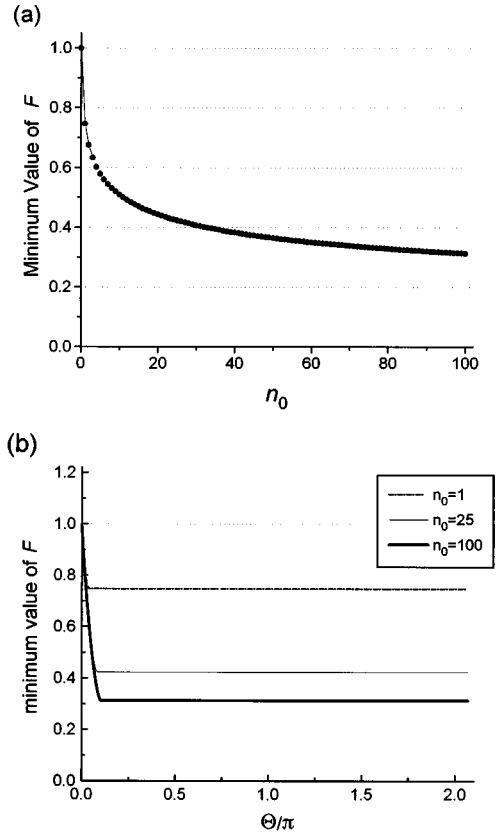

FIG. 8. The minimum value of the Fano factor is plotted as a function of (a) the initial mean photon number n_0, and (b) the nonlinear parameter Θ under an appropriate choice of N and ϕ_{ij}. In (b), three cases for $n_0=1$, 25, and 100 are plotted.

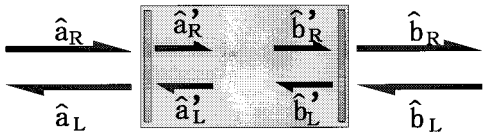

FIG. 9. Definition of the operators in the case of finite partial reflection at surfaces of the materials. The prime stands for the photon operators inside the medium.

The minimum value of the Fano factor, given by a local minimum in Fig. 7, is plotted as a function of n_0 in Fig. 8(a), and of Θ in Fig. 8(b). These show that F becomes smaller as n_0 increases. Recalling that the QPA squeezing is independent of n_0, *simultaneously optimal* squeezing of the QPA and the photon number is always possible for given n_0 and Θ with use of the modulation pumping.

IV. EFFECTS OF SURFACE REFLECTION

In previous sections, we assumed perfect phase-conjugate reflection, i.e., no normal reflection of light at surfaces of the phase conjugators. In actual experiments, however, the incident light is partly reflected at interfaces between vacuum and the nonlinear media before the light experiences the optical nonlinearities in the materials. In this section, we will take this effect into account, which can also be treated by the transfer-matrix method.

We shall first consider the single phase-conjugator model (Yurke's model) for simplicity; we pay attention only to the ith material. At a surface, as shown in Fig. 9, the operator relations become

$$\begin{pmatrix} \hat{a}_L \\ \hat{a}_R \end{pmatrix} = \frac{1}{\sqrt{T}} \begin{pmatrix} 1 & \sqrt{R} \\ \sqrt{R} & 1 \end{pmatrix} \begin{pmatrix} \hat{a}'_L \\ \hat{a}'_R \end{pmatrix}, \tag{32}$$

$$\begin{pmatrix} \hat{b}'_L \\ \hat{b}'_R \end{pmatrix} = \frac{1}{\sqrt{T}} \begin{pmatrix} 1 & -\sqrt{R} \\ -\sqrt{R} & 1 \end{pmatrix} \begin{pmatrix} \hat{b}_L \\ \hat{b}_R \end{pmatrix}, \tag{33}$$

where $0 \leqslant T \leqslant 1$ and $0 \leqslant R = 1-T \leqslant 1$ are the transmittance and reflectivity at a surface, respectively. We further assume that T and R are the same for all surfaces of all phase conjugators. Equation (12) is now changed to

$$\begin{pmatrix} \hat{a}'_L \\ [\hat{a}'_R]^\dagger \end{pmatrix} = \frac{1}{\mu_i} \begin{pmatrix} 1 & \nu_i \\ -\nu_i^* & 1 \end{pmatrix} \begin{pmatrix} \hat{b}'_L \\ [\hat{b}'_R]^\dagger \end{pmatrix}. \tag{34}$$

We use 4×4 matrices to describe the input-output relation of the single-phase conjugator, taking into account the surface reflection as

$$\tilde{\mathbf{A}} = \mathbf{I}_L \tilde{\mathbf{M}}_i \mathbf{I}_R \tilde{\mathbf{B}} \equiv \tilde{\mathbf{M}}_i^* \tilde{\mathbf{B}}, \tag{35}$$

where $\tilde{\mathbf{A}} = {}^t(\hat{a}_L, \hat{a}_L^\dagger, \hat{a}_R, \hat{a}_R^\dagger)$, $\tilde{\mathbf{B}} = {}^t(\hat{b}_L, \hat{b}_L^\dagger, \hat{b}_R, \hat{b}_R^\dagger)$:

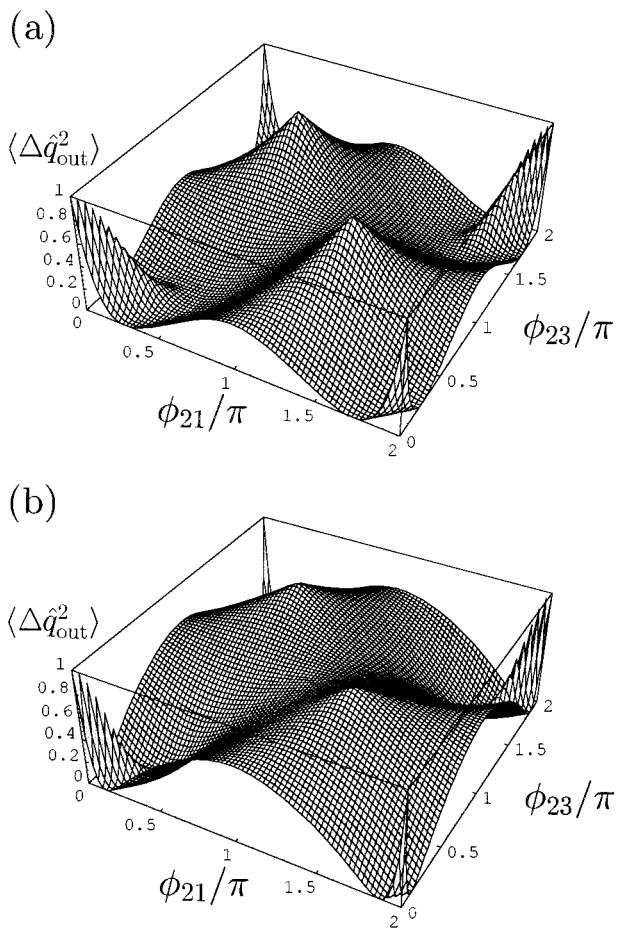

FIG. 10. The QPA variance $\langle \Delta \hat{q}^2_{\rm out} \rangle$ is plotted as a function of two pump phase differences, ϕ_{21} and ϕ_{23}, in the case of $N=3$ for (a) $R=0.2$ and (b) $R=0.5$. The nonlinear parameter and phase changes are chosen to be $\Theta=\frac{1}{2}\pi$ (i.e., $\theta=\frac{1}{6}\pi$) and $\vartheta_{12}=\vartheta_{23}=2m\pi$, respectively.

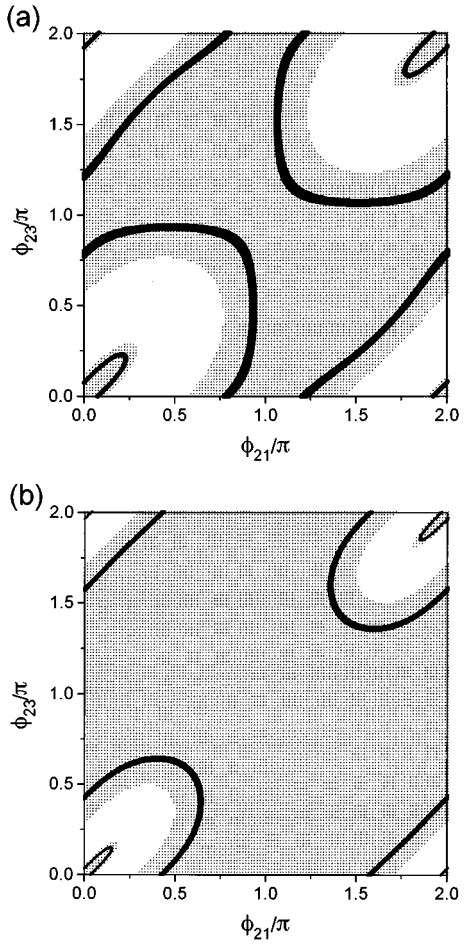

FIG. 11. The Fano factor is calculated on the plane of (ϕ_{21},ϕ_{23}) in the case of $N=3$ for $\Theta=\frac{1}{2}\pi$, $n_0=25$, and $\phi_{\rm SA}=\frac{1}{2}\pi$. The reflectivity is chosen to be (a) $R=0.2$ and (b) $R=0.5$. In dotted regions, the photon statistics is sub-Poissonian $(F<1)$. The Fano factor becomes minimum on the solid lines. The phase changes are chosen to be $\vartheta_{12}=\vartheta_{23}=2m\pi$.

$$\mathbf{I}_L=\frac{1}{\sqrt{T}}\begin{pmatrix} 1 & 0 & \sqrt{R} & 0 \\ 0 & 1 & 0 & \sqrt{R} \\ \sqrt{R} & 0 & 1 & 0 \\ 0 & \sqrt{R} & 0 & 1 \end{pmatrix}, \tag{36}$$

$$\tilde{\mathbf{M}}_i=\frac{1}{\mu_i}\begin{pmatrix} 1 & 0 & 0 & \nu_i \\ 0 & 1 & \nu_i^* & 0 \\ 0 & -\nu_i & 1 & 0 \\ -\nu_i^* & 0 & 0 & 1 \end{pmatrix}, \tag{37}$$

$$\mathbf{I}_R=\frac{1}{\sqrt{T}}\begin{pmatrix} 1 & 0 & -\sqrt{R} & 0 \\ 0 & 1 & 0 & -\sqrt{R} \\ -\sqrt{R} & 0 & 1 & 0 \\ 0 & -\sqrt{R} & 0 & 1 \end{pmatrix}. \tag{38}$$

Here $\tilde{\mathbf{M}}_i^*$ means an effective matrix describing the FWM nonlinearity in the ith material.

When the normal reflection at surfaces is involved, a output beam becomes a mixture of the phase-conjugate-reflection light and the normal-reflection one. Therefore, the input-output characteristics depend on the phase change ϑ_{ij} due to free propagation in the vacuum between the ith and $j(=i\pm1)$th phase conjugators. This is in contrast to the discussion in Sec. II without the surface reflection. Thus we have to insert the 4×4 vacuum matrix $\tilde{\mathbf{V}}_{ij}$ into effective matrices, $\tilde{\mathbf{M}}_i^*$ and $\tilde{\mathbf{M}}_j^*$, when $N\geqslant2$. Here $\tilde{\mathbf{V}}_{ij}$, which describes the free propagation, is written explicitly as

$$\tilde{\mathbf{V}}_{ij}=\begin{pmatrix} e^{i\vartheta_{ij}} & 0 & 0 & 0 \\ 0 & e^{-i\vartheta_{ij}} & 0 & 0 \\ 0 & 0 & e^{-i\vartheta_{ij}} & 0 \\ 0 & 0 & 0 & e^{i\vartheta_{ij}} \end{pmatrix}. \tag{39}$$

When $N\geqslant2$ in our cascade model, the total 4×4 transfer matrix $\tilde{\mathbf{T}}$ of the total system is given by alternately producing the effective matrices $\tilde{\mathbf{M}}_i^*$ and the vacuum matrices $\tilde{\mathbf{V}}_{ij}$ as

$$\tilde{\mathbf{T}}=\left[\prod_{i=1}^{N-1}\tilde{\mathbf{M}}_i^*\tilde{\mathbf{V}}_{i,i+1}\right]\tilde{\mathbf{M}}_N^*=\left[\prod_{i=1}^{N-1}\mathbf{I}_L\tilde{\mathbf{M}}_i\mathbf{I}_R\tilde{\mathbf{V}}_{i,i+1}\right]\mathbf{I}_L\tilde{\mathbf{M}}_N\mathbf{I}_R\,. \tag{40}$$

Here we assumed that the free space between the Nth phase conjugator at the right end and the perfect mirror is neglected. When $\vartheta_{ij}=2m\pi$ ($m=0,1,2,\ldots$), in particular, Eq. (40) becomes a simpler form of

$$\tilde{\mathbf{T}}=\mathbf{I}_L\left[\prod_{i=1}^{N}\tilde{\mathbf{M}}_i\right]\mathbf{I}_R\,, \tag{41}$$

and then we can evaluate the transfer matrices analytically. Without loss of generality, we assume $\vartheta_{ij}=2m\pi$ hereafter because $\vartheta_{ij}\neq 2m\pi$ merely shifts the origin of ϕ_{ij} leading to no qualitative change in the squeezing properties.

If the (i,j) component of the 4×4 transfer matrix $\tilde{\mathbf{T}}$ is written as $(\tilde{\mathbf{T}})_{ij}=\tilde{t}_{ij}^{(N)}$ for $i,j=1,\ldots,4$, the input-output relation is expressed as

$$\hat{a}_{\rm out}=\frac{\tau_1^{(N)}[\tau_3^{(N)}]^*-\tau_2^{(N)}[\tau_4^{(N)}]^*}{|\tau_3^{(N)}|^2-|\tau_4^{(N)}|^2}\hat{a}_{\rm in}+\frac{\tau_2^{(N)}\tau_3^{(N)}-\tau_1^{(N)}\tau_4^{(N)}}{|\tau_3^{(N)}|^2-|\tau_4^{(N)}|^2}\hat{a}_{\rm in}^\dagger$$

$$\equiv\tilde{\mu}_{\rm PCC}^{(N)}\hat{a}_{\rm in}+\tilde{\nu}_{\rm PCC}^{(N)}\hat{a}_{\rm in}^\dagger, \tag{42}$$

$$\tau_1^{(N)}\equiv\tilde{t}_{11}^{(N)}+\tilde{t}_{13}^{(N)}\,, \tag{43}$$

$$\tau_2^{(N)}\equiv\tilde{t}_{12}^{(N)}+\tilde{t}_{14}^{(N)}\,, \tag{44}$$

$$\tau_3^{(N)}\equiv\tilde{t}_{31}^{(N)}+\tilde{t}_{33}^{(N)}\,, \tag{45}$$

$$\tau_4^{(N)}\equiv\tilde{t}_{32}^{(N)}+\tilde{t}_{34}^{(N)}\,. \tag{46}$$

Explicit forms of these matrix elements will be given elsewhere. This is another general formula obtained in this paper. The unitarity condition $|\tilde{\mu}_{\rm PCC}^{(N)}|^2-|\tilde{\nu}_{\rm PCC}^{(N)}|^2=1$ also holds in this case. Then, using $\tilde{\mu}_{\rm PCC}^{(N)}$, we can evaluate, e.g., the QPA variance $\langle\Delta\hat{q}_{\rm out}^2\rangle$ and the Fano factor F to discuss the squeezing properties in the case of finite surface reflection.

Figures 10(a) and 10(b) show the normalized QPA variance $\langle\Delta\hat{q}_{\rm out}^2\rangle$ in the $N=3$ case for $R=0.2$ and 0.5 as a function of the phase differences ϕ_{21} and ϕ_{23}. Comparing these figures with Fig. 4(a), one finds that the QPA variance becomes larger (worse squeezing) when R increases. However, we can still obtain the infinite QPA squeezing ($\langle\Delta\hat{q}_{\rm out}^2\rangle=0$) by choosing appropriate pump phase differences even when $R>0$. The photon-number squeezing can also be obtained; Figs. 11(a) and 11(b) indicate the possibility of sub-Poissonian statistics even when $R>0$.

V. CONCLUSIONS

We proposed an improved scheme for generation of the squeezed states, extending Yurke's single-phase-conjugator model to the cascade one. It was shown theoretically that not only QPA squeezing of light but also photon-number squeezing take place in our cascade model, and the fluctuation characteristics were analytically discussed. In particular, we investigated in detail the dependence of squeezing features on the phases of the pumping beams and on the number of FWM materials, clarifying differences from Yurke's results. We stress that the pumping phase differences, which are new control parameters easily tunable in actual experiments, effectively alter the squeezing characteristics. Thus finer controllability of the squeezing characteristics is obtained by our cascade phase-conjugator scheme with the modulation pumping technique. Moreover, normal reflection of light at surfaces of phase-conjugate materials is shown to reduce the squeezing. Even for the case of finite normal reflection, the infinite QPA squeezing is still possible with the best use of the modulation pumping. Thus we can independently control the QPA squeezing and the photon-number squeezing to yield the simultaneously optimal squeezing in terms of both.

ACKNOWLEDGMENTS

In the early stage of this work the authors were indebted to N. Hatakenaka for initiation of these kinds of problems. The authors also thank S. Kurihara, K. Nakamura, Y. Takane, and T. Maki for fruitful discussions. This work was supported by a Grant-in-Aid for Scientific Research on Priority Areas, ''Mutual Quantum Manipulation of Radiation Field and Matter,'' from the Ministry of Education, Science, Sports and Culture of Japan.

[1] See, e.g., P. Meystre and M. Sargent III, *Elements of Quantum Optics* (Springer-Verlag, Berlin, 1991); D. F. Walls and G. J. Milburn, *Quantum Optics* (Springer-Verlag, Berlin, 1994).
[2] L. A. Wu, H. J. Kimble, J. L. Hall, and H. Wu, Phys. Rev. Lett. **57**, 2520 (1986).
[3] E. S. Polzik, J. Carray, and H. J. Kimble, Appl. Phys. B: Photophys. Laser Chem. **55**, 279 (1992).
[4] H. P. Yuen and J. H. Shapiro, Opt. Lett. **4**, 334 (1979).
[5] R. E. Slusher, L. Hollberg, B. Yurke, J. C. Mertz, and J. F. Valley, Phys. Rev. A **31**, 3512 (1985).
[6] R. E. Slusher, L. W. Hollberg, B. Yurke, J. C. Mertz, and J. F. Valley, Phys. Rev. Lett. **55**, 2409 (1985).
[7] M. Kitagawa and Y. Yamamoto, Phys. Rev. A **34**, 3974 (1986).
[8] B. Yurke, Phys. Rev. A **29**, 408 (1984).
[9] J. Bajer and J. Perina, Opt. Commun. **85**, 261 (1991).
[10] G. S. Agarwal, A. L. Gaeta, and R. W. Boyd, Phys. Rev. A **47**, 597 (1993).
[11] M. Y. Lanzerotti, A. L. Gaeta, and R. W. Boyd, Phys. Rev. A **51**, 3182 (1995).
[12] N. Hatakenaka, T. Ogawa, and S. Kurihara, Phys. Lett. A **204**, 223 (1995).